Available online at www.sciencedirect.com

ScienceDirect

Energy Procedia 4 (2011) 3063–3070

Energy Procedia

www.elsevier.com/locate/procedia

GHGT-10

Corrosion of transport pipelines for CO_2 – effect of water ingress

Arne Dugstad[a], Bjørn Morland[a] and Sigmund Clausen[b] 1*

[a] *Institute for Energy Technology (IFE), PO. Box 40, 2027 Kjeller, Norway*
[b] *Gassco AS,* PO. Box 93, N-5501 Haugesund, Norway

Abstract

Both field experience and lab data indicate that the corrosion rate of carbon steel in pure dense phase CO_2 is near zero if no free water is present. The question is whether this also applies when other contaminants like SO_x, NO_x, H_2S and O_2 are present in moderate amounts.

In a pipeline network with different types of CO_2 sources, the commingling of streams with various impurities can give a very complex mixture, and side reactions like oxidation and decomposition of impurities can be foreseen. An important issue is how the contaminants partition between the various phases during pressure reduction and when free water is present. The corrosion mechanisms under these conditions are not well understood, and it becomes more and more uncertain what will happen when the concentration of contaminants including water increases. The paper addresses these issues and discusses recent corrosion flow loops and autoclaves results obtained in an ongoing sub-sea CO_2 transmission pipeline project.

Keywords: CCS; corrosion; water; O_2; SO_2; depressurisation

1. Introduction

Following CO_2 capture it is possible to treat CO_2 to near 100% purity in the gas conditioning process. However, in most cases it is preferable to have less rigid specifications to reduce both energy and capital costs. Furthermore, there are currently no recognized specifications for the CO_2 quality required for pipeline transport, and it is possible that when specifications eventually are established, the required CO_2 quality may vary depending on the end target (EOR, storage in aquifers or other storage) and legislation differences. The main technical constraint will be the maximum allowable impurity content in CO_2 to be injected or the impurities that can be allowed from a corrosion and safety point of view (rupture) during pipeline or ship transport. A tentative recommendation based on work that has been done in the European project "ENCAP" has been suggested in the DYNAMIS project[1] and Alstom has compiled and published[2] reference data showing the tolerances for various contaminants with respect to EOR, H&S, corrosion and storage. Large variations in the composition are foreseen. This is reasonable as the impurities in the

* Corresponding author. Tel.: +47 63 80 62 63; fax: +47 63 80 62 58.
E-mail address: arne.dugstad@ife.no.

doi:10.1016/j.egypro.2011.02.218

CCS stream will depend on the fuel type, the energy conversion process (post-combustion, pre-combustion or oxyfuel) and the capture process.

When pipeline design philosophy for CO_2 transportation is discussed it is commonly accepted that the CO_2 should be sufficiently dry to prevent drop-out of a separate aqueous phase in any part of the pipeline, as free water can give both corrosion and hydrate formation. It is however no consensus on what the actual target for the maximum water concentration should be. It has been argued that full dehydration down to 50 ppm should be applied. This limit has been specified for the first CO_2 pipelines in the USA and for the Snøhvit pipeline in Norway. Other specifications are less conservative (500 ppm) as in the DYNAMIS project.

The precipitation of an aqueous phase will be very much dependent on the impurities in the CO_2. If glycol, SO_x and NO_x are present they will dissolve readily in water and give an aqueous phase at a much lower water concentration than the solubility limits reported for pure CO_2 and CO_2 contaminated with hydrocarbons [1,3,4]. If a system is partly depressurised a two phase gas/liquid system forms and impurities will partition between the two phases. When the solubility in the gas phase is lower than in the liquid phase an accumulation of the impurities is expected in the remaining liquid phase. The accumulation of impurities during depressurisation can have a large effect on corrosion as the water and impurities form a separate corrosive phase.

Regardless of the target concentration accidental ingress of water in a complex network of pipelines might happen. If dry CO_2 continues to flow after a water incident, it is assumed that the water will be dissolved quickly and not seriously threaten the integrity of the pipeline. Continuous water ingress or long lasting shut down after water ingress will give a quite different situation. At shut down it might be necessary to remove the water in the pipeline. Water removal includes depressurization of the pipeline and experience from existing pipelines indicates that this can take weeks. The acceptable response time after water contamination will be system specific and depend on the corrosion rate and corrosion allowance. Presently, the corrosion rate in a pipeline suffering from accidental water ingress cannot be estimated accurately due to lack of corrosion data.

Institute for Energy Technology is currently running a corrosion study for a planned sub-sea CO_2 transmission pipeline in Norway. The CO_2 specification is shown in Table 1. A conservative approach has been adopted to ensure the integrity of the pipeline system, implying strict requirements to the content of impurities in the CO_2 stream. These requirements imply a need for implementing additional and costly processing equipment, like processes for H_2O drying and O_2 removal downstream of the capture plant to enable fulfilment of the CO_2 specification. In the current study an amine process for capturing and cleaning the CO_2 has been assumed. Some preliminary results from the study are presented and discussed in the paper together with previously published work.

Table 1 CO_2 specification

N_2	<0.04 mol %
H_2O	< 50 ppm
H_2S	< 100 ppm
O_2	< 200 ppm
NH_3	Trace
Amine	Trace
CO_2	Balance

2. Experimental approach

Static corrosion experiments were run in small 140-200 ml autoclaves. The corrosion reaction consumes water corresponding to about 40 ppm (mass) per week per cm^2 when the corrosion rate is 1 mm/year. Small samples (0.7 cm^2) were therefore used in experiments with low water content. The corrosion rate was determined by weight loss and in addition iron counts when the experiments was run with a free water phase.

Dynamic corrosion experiments were run in a 180 bar 6.5 litre dense phase Hastelloy C flow loop. A pump was used to circulate the liquid water phase which was in contact with the dense phase CO_2 in a water-CO_2 separator upstream the pump. One or two tubular test specimens with 7 mm inner diameter and maximum length 50 mm were mounted in each of the two test sections. Electrochemical techniques could not be used as the water phase had too low conductivity and the corrosion rate was therefore measured from weight loss and the accumulation rate of dissolved corrosion products in the water phase

The test specimens were machined from a Ferrite-pearlite X65 pipeline steel and ground with 1000 mesh paper. The composition(wt-%) in addition to **Fe** was: **C** (0.08), **Si** (0.25), **Mn** (1.54), **S** (0.001), **P** (0.019), **Cr** (0.04), **Ni** (0.05), **V** (0.095), **Mo** (0.01), **Cu** (0.02), **Al** (0.038), **Sn** (0.001), **Nb** (0.043)

3. Results of corrosion experiments

3.1. Corrosion tests at stagnant conditions and low water content (< 500 ppm)

Steel specimens were exposed in dense phase CO_2 with various amounts of H_2O, SO_2 and O_2. The test conditions and the results are summarized in Table 2. No corrosion attack was registered in pure CO_2 and water and in the experiment with O_2. However, corrosion was observed in the experiments with added SO_2. The test specimens were blackish after exposure and the surface was covered with a thin corrosion film, see example in Figure 1. EDS analyses of the film indicated the formation of $FeSO_4$. The weight loss corrosion rate was about 0.01 mm/year at the highest SO_2 content.

Table 2 Autoclave tests carried out at low water concentration, < 500 ppm (mass)

Exp. No:	IFE 3a	IFE 3b	IFE 3c	IFE 3d
Temp, °C	20	20	20	20
Pressure, bar	~100	~100	~100	~100
H_2O, ppm	500	500	200	200
O_2 , ppm	0	200	100	100
SO_2, ppm	0	0	1000	200
Exposure, days	30	30	7	7
Average Corrosion rate, mm/y	No attack	No attack	0.01	<0.01

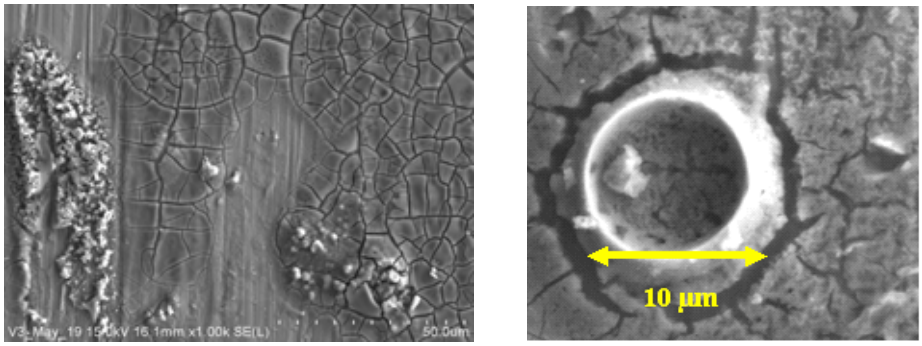

Figure 1 The morphology of the surface film formed on the steel sample exposed in experiment IFE 3c with 1000 ppm SO_2.

3.2. Corrosion tests at stagnant conditions and 50 vol% water

Eight autoclave experiments were run with dense phase CO_2 and 50 volume % water at various temperatures with and without oxygen (100-500 ppm). Test conditions and results are shown in Table 3. Protective corrosion product films formed on the steel surface in exp IFE-1d and 2c. The corrosion rates measured in the other experiments are plotted as a function of temperature in Figure 2. It is seen that the corrosion rate increases with increasing temperature. Film stripping and analyses of the steel specimens after the exposure showed that the amount (weight) of corrosion product sticking to the surface corresponded to less than 3 µm compact film assuming a density of 3 g/ml. The actual film was somewhat thicker (confirmed with SEM), porous and did not offer much protection. Addition of O_2 increased the corrosion rate 50-120 % in the experiments without protective film formation.

Table 3 Autoclave tests carried out with a free water phase (50 vol% water).

Exp. No:	IFE-1a	IFE-1c	IFE-1d	IFE-1e	IFE-2a	IFE-2b	IFE-2c	IFE-1b
Temp, °C	10	20	50	50	10	20	50	20
Pressure, bar	~100	~100	~100	~100	~100	~100	~100	~100
O_2 , ppm	0	0	0	0	200	100	200	0
H_2O, vol%	50	50	50	50	50	50	50	50
Exposure, days	13	14	14	14	13	14	18	3
Volume/surface ratio, cm^3/cm^2	16	16	16	16	100	16	100	16
Fe^{2+} (end), ppm	748	900	300	90	320	500	310	490
Estimated start pH	3.0-3.2	3.0-3.2	3.0-3.2	3.0-3.2	3.0-3.2	3.0-3.2	3.0-3.2	3.0-3.2
Estimated final pH	~4.7	~4.8	~4.3	~3.8	~4.3	~4.5	~4.3	~4.5
Type of attack	Uniform						Localized	Uniform
Average corrosion rate, mm/y	0.5	0.8	0.5	2.7	1.2	1.3	0.6	1.1
Pitting rate, mm/y	-	-	-	-	-	-	17	-
Film thickness, µm	2.3	3	38.7	3	0.5	3.3	107.6	1.6

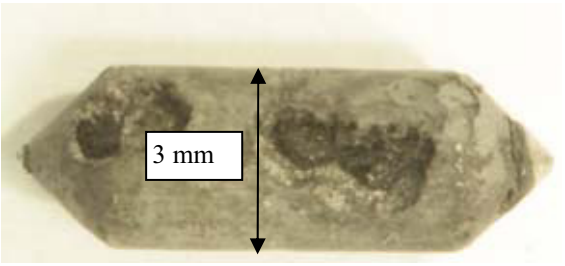

Figure 3 Corroded sample, IFE-2c.

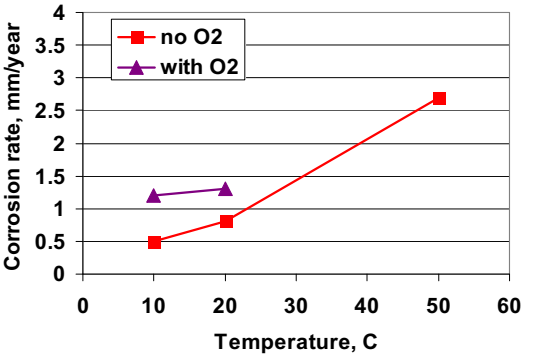

Figure 2 Corrosion rate as a function of temperature.

When the iron content in the solution was above the solubility limit for iron carbonate formation, corrosion products precipitated on the surface in the 50 °C experiments. A hard and black 40 µm thick corrosion films formed in the experiment (exp IFE-1d) without oxygen and the average corrosion rate was significantly reduced compared to experiment IFE-1e with lower concentration of dissolved iron. The surface was covered with a smooth layer of $FeCO_3$ crystallites and no localised corrosion attack could be seen when the film was stripped off.

The dissolved iron content in the O_2 experiment was much lower than in the experiment without O_2 because O_2 reacts with Fe^{2+} and forms iron oxides. The water phase was orange (rusty) when the experiment was terminated. The lower iron content probably destabilizes the iron carbonate film giving a local failure of the protective corrosion film where the deep localised attack seen in Figure 3 could develop. The depth of the attack corresponded to a corrosion rate of about 16 mm/year.

3.3. Corrosion tests under flowing conditions

The loop experiments were run at 100 bar CO_2 pressure and 13 and 50 °C respectively. The water phase that was mixed with dense phase in the separator upstream the pump was circulated at 1 and 3 m/s. When the temperature was below 11-12 °C, hydrate formed and the flow stopped. The hydrate was dissolved again when the temperature was increased to 12-13 °C.

The measured corrosion rates plotted as a function of flow are shown in Figures 4. It is seen that increasing the flow velocity increased the corrosion rate substantially. The effect was most pronounced at 50 °C. The plotted corrosion rates were measured after about 10-20 days exposure at 13 °C and 2-4 days at 50 °C. The iron content was 100-400 ppm and the estimated pH in the range 3.9-4.4. The corrosion rate was about 10-20 % higher in the beginning of the exposure when the steel was fresh abraded and the iron content less then 100 ppm. The corrosion rate increased about 50 % when 1000 ppm O_2 was added to the dense phase CO_2 in the beginning of the exposure. The O_2 was consumed during the exposures and the concentration was about 350 ppm when the experiment was stopped.

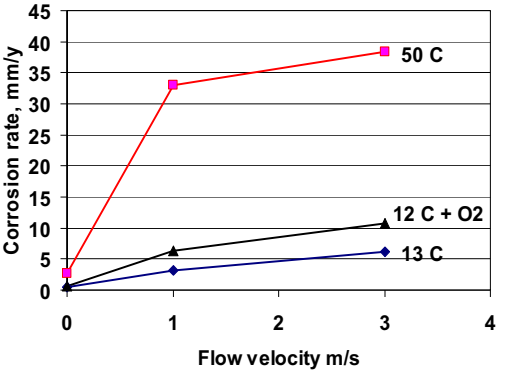

Figure 4 Corrosion rate as a function of flow velocity.

Almost no corrosion products precipitated on the steel surface in the 13 °C experiments. The film thickness estimated from the weight loss after stripping corresponded to less than 3 µm. A porous 10-30 µm thick film formed in the 50 °C experiment. The film offered little protection. The film was thinnest at the highest flow velocity indicating that it was partly removed mechanically by the flow.

4. Changes in the corrosivity after depressurisation

Partitioning and depressurisation experiments were run with dense phase CO_2 mixed with O_2, H_2S and SO_2 respectively at 20 °C. The test autoclaves were completely filled with the mixture. When the system had equilibrated, CO_2 was slowly vented at 20 °C via the gas phase until all liquid CO_2 had been converted to gas. Samples were taken frequently from both the gas and the liquid phases and analysed with gas chromatography.

Water could not be analysed directly, but was converted to acetylene by a reaction with CaC_2. The measured ratio (partitioning coefficient) between the concentration in the gas phase and the liquid phase is shown in Table 4. The ratio was less than 1 for H_2O, SO_2 and H_2S and larger than 1 for O_2. The measured concentration (together with simulations, solid lines) of H_2S and O_2 in the liquid and the gas phases has been plotted as a function of CO_2 venting in Figure 5.

Table 4 Partitioning coefficients

Impurity	Partitioning coefficient (gas/liquid)
O_2	2.5-3
H_2S	0.6-0.8
SO_2	0.04-0.06
H_2O	0.2-0.3

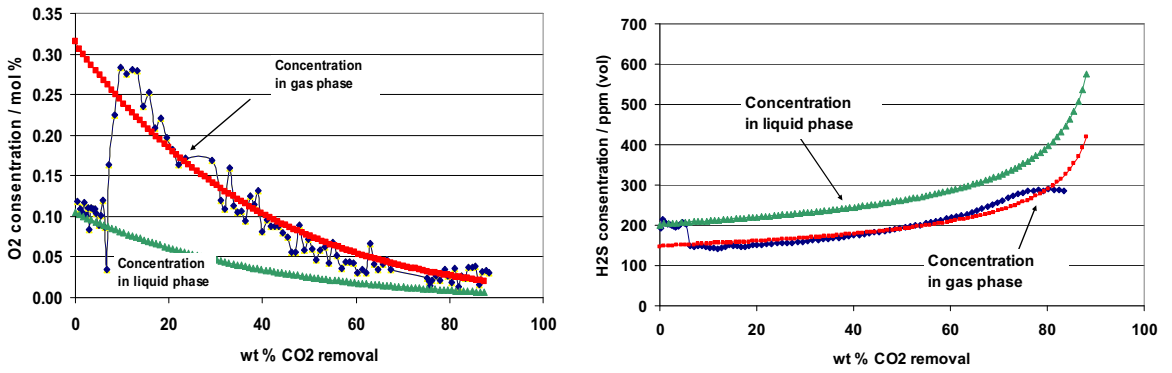

Figure 5 Partitioning of O_2 (left) and H_2S (right) as a function of venting

5. Discussion

5.1. Corrosion in dense phase CO_2 with low water content.

It seems to be generally accepted that the corrosion rate is insignificant when the water content is well below the solubility limit. Both field experience[5, 6, 7] and previously reported lab experiments[8, 9, 10] indicates this. Chevron did some experimental work[9, 10] in the 1970's and concluded "No evidence of pitting or general corrosion attack. Corrosion rates were less than 0.02 MPY (0.0005 mm/year)." The water content in these experiments was 1000 ppm, the H_2S concentration 800 ppm and the temperature about 3 and 23 °C respectively.

The present study supports that corrosion does not take place in pure CO_2 or CO_2 with oxygen when the water content (500 ppm) is far below the reported water solubility limit for pure CO_2. Corrosion occurred at very low water concentration (200 ppm) when the system was contaminated with SO_2. When SO_2, water and O_2 are present sulphuric acid (H_2SO_4) might form. The minimum water concentration required for H_2SO_4 formation is not known, but the presence of $FeSO_4$ on the corroded surface indicates that the reaction occurred. No data has been found on the solubility of sulphuric acid in dense phase CO_2. The solubility seems to be low as the corroded surfaces had a film formation morphology that indicated that small droplets attached to the surface, see Figure 1. The experiments were run under stagnant conditions and only a few % of the potentially available $H_2O/SO_2/H_2SO_4$ was consumed. It can be questioned whether the corrosion rate will be much higher under flowing conditions, as dissolved H_2SO_4 has the possibility to be transported to the surface at a much higher rate.

5.2. Corrosion in dense phase CO_2 when water forms a separate phase

When the steel corrodes in pure CO_2 and water, the dissolved iron content increases, and that gives a subsequent increase in pH as illustrated in Figure 6. The iron/pH response was estimated with MultiScale[14] at 100 bar CO_2 and 13 and 50 °C respectively. The two dashed vertical lines indicates when the solubility product is larger than 1 (supersaturation).

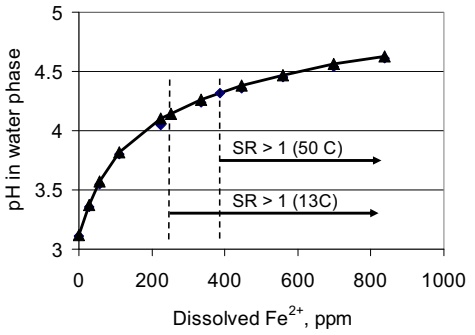

Figure 6 pH estimated with MultiScale[14]

The increase in the iron concentration will depend on the corrosion rate and the steel surface to water volume ratio. When the Fe^{2+} solubility limit is exceeded iron carbonate can precipitate. The precipitation rate is very temperature dependent, and it is not expected much precipitation in corrosion tests lasting less than 1 month when the temperature is below 30 °C[11]. This was confirmed in the present study where the dissolved Fe^{2+} concentration was far above the expected solubility limit in all the 4 to 20 °C experiments. The situation was quite different at 50 °C where the amount of corrosion products on the steel surface varied strongly with the dissolved iron concentration in the solution. Almost no corrosion film was detected on the steel surface in experiment IFE-1e where the iron content was kept below the solubility limit and the corrosion rate was high, 2.7 mm/year. A thick corrosion product film formed when the iron content increased above the solubility limit (experiments IFE-1d and IFE-2c) and the film gave full protection in the experiment without O_2. It should be noted that since the initial corrosion rate is much higher in the experiments where protective corrosion product films are formed, the final corrosion rate will be much lower that the average corrosion rate reported in the table.

The protective film can be destabilised if the iron content is reduced in the solution. This happened in the experiment with O_2 where the dissolved iron content was lower than in the O_2-free experiment. The lower concentration is attributed to the reaction between O_2 and Fe^{2+} forming iron oxides. The film obviously failed in experiment IFE-2c and a deep localised attack developed. The depth of the attack corresponded to a penetration rate

of 16 mm/year. The corrosion rate was much higher than in the experiment without O_2, and that indicates that the O_2 also attacks the steel directly and not only reacts with the corrosion products.

The measured corrosion rates when protective films did not form under stagnant conditions were slightly lower than those published in a previous study[12,13]. These experiments were done with a slow circulation (<< 1m/s) of the water phase and the comparison of the results shows how sensitive the corrosion rate is when it comes to flow and convection.

5.3. Changes in the corrosivity after depressurisation

The partitioning coefficient was less than 1 for H_2O, SO_2 and H_2S and the concentration of these impurities will therefore increase in the liquid phase when the system is depressurised via the gas phase as shown in Figure 5. The effect is opposite for O_2 which has a partitioning coefficient of > 2.

A simple mass balance model for accumulation of impurity during depressurisation has been developed, and the model has been used to estimate the accumulation rates in the dense phase and the change in the impurity concentration in the venting gas as a function of vented CO_2. The simulations have been compared with the actual measurements in Figure 5, and the fit is very good. The model uses the partitioning coefficient and the initial concentration as input, and the output is the concentration in the remaining liquid phase and gas phase as a function of evaporated CO_2.

The accumulation of impurities during depressurisation is expected to have a large effect on corrosion. The water concentration can increase beyond the saturation limit and form a corrosive liquid highly concentrated in all the impurities that has a partitioning coefficient lower than 1. The preliminary partitioning coefficient measured for SO_2 is very low and the amount of H_2SO_4 that can accumulate in an aqueous phase after a pressure reduction might be significant. If the aqueous phase after depressurisation accumulates in low spots it can be foreseen severe local corrosion attack. An actual depressurisation will most likely be done at a much lower temperature than the 20 °C used for the present partitioning and depressurisation testing. More data are required in order to predict accumulation rates over a wider temperature range and for other impurities including glycol, amines, CO and NO_x.

5.4. CO_2 corrosion in oil and gas production vs. CCS streams

Experiments have shown that the corrosion rate increases with increasing temperature, that $FeCO_3$ corrosion product films form when the solubility is exceeded and that the corrosion film can fail and give high localised corrosion rates. The observations seem to follow very much the trends seen at lower CO_2 partial pressure in oil and gas production.

The flow dependency was more pronounced than usually seen at lower CO_2 partial pressure. The corrosion rate increased more than 10 times going from stagnant conditions to 3 m/s. The large flow effect can be attributed to the lower pH. The two main cathodic reactions in a pure CO_2 -water system are:

$$H^+ + e^- \rightarrow \tfrac{1}{2} H_2 \quad (1)$$

$$H_2CO_3 + e^- \rightarrow \tfrac{1}{2} H_2 + HCO_3^- \quad (2)$$

Equations 1 and 2 are the overall reaction routes and do not show the detailed mechanisms of the proton reduction. The relative contribution from each of these reactions depends amongst other on the concentrations of the reactants, temperature, pH and convection. In solutions with strong acids, which are fully dissociated, the rate of hydrogen evolution occurs according to equation 1 and cannot exceed the rate at which H^+ ions are transported to the surface from the bulk solution (mass transfer limit). Its contribution to the corrosion rate is small above pH 5, a typical pH in formation water associated with oil and gas production. Then H_2CO_3 serves as an additional source of H^+ ions that enables the hydrogen evolution reaction to proceed at a much higher rate than in a solution of a strong

acid at the same pH. The pH in the dense phase CO_2 experiments has been in the range 3.1 - 4.5, and the flow dependent contribution from the H^+ reaction is expected to become more important than usually seen in oil and gas production environments where the pH is higher.

Essential differences between the CCS stream and traditional gas and oil production include:

- The much higher CO_2 pressure gives a lower pH, typically one unit. This should give a higher solubility of corrosion products and more H^+ ions that can corrode the steel. The much higher CO_2 concentration should give more H_2CO_3 and thus increase the potential corrosion rate when a separate aqueous phase is present.
- Presence of large amounts of O_2 will give an additional cathodic reaction that can accelerate the corrosion.
- If the CCS stream contains SO_2 and/or NO_x, these products will dissolve in the aqueous phase and give a reduction in pH, increased amount of H^+ that can be used for corrosion and increased solubility of corrosion products. The higher solubility reduces the likelihood for formation of protective corrosion product films.
- It is not clear whether a CCS stream will contain organic acids as they have not been included in any of the specifications. There will be a lot of formates and acetate (degradation products) in the amines usually used in the capture process, and if some of the amines follow the CCS streams organic acids should also be expected.
- Presence of large amounts of O_2 will oxidize the corrosion products and reduce the pH.

Acknowledgment

The authors would like to acknowledge Gassco AS for financial and technical support for parts of the presented work.

References

[1] E. de Visser et al. Dynamis CO_2 quality recommendations, International Journal of Greenhouse Gas Control 2 (2008) p. 478-484
[2]. IEAGHG Int. Oxy-Combustion Network, Yokohama, Japan, 5-6 March, 2008
[3] K. Y. Song, R. Kobayashi, SPE Formation Evaluation (1987) :p. 500
[4] M. B. King, A. Mubarak, J. D. Kim, T. R. Bott, J. Supercrit. Fluids 5, (1992) :p. 296
[5] J.M.West, "Design and Operation of a Supercritical CO_2 Pipeline-Compression System Sacroc Unit, Scurry County, Texas", SPE paper no. 4804, 1974.
[6] L.E.Newton, CORROSION/84, Paper no. 67, NACE International, Houston, 1984.
[7] T.E.Gill, "Canyon Reef Carriers, Inc. CO_2 Pipeline: Description and 12 Years of Operation", ASME Energy-Source Technol. Conf, Pipeline Eng. Symp., p. 59, 1985.
[8] W.A.Propp, T.E.Carleson, C.M.Wai, P.R.Taylor, K.W.Daehling, S.Huang, M. Abdel-Latif, "Corrosion in Supercritical Fluids", US Department of Energy report DE96014006, Washington DC, 1996.
[9] F.W.Schremp, G.R.Roberson, "Effect of Supercritical Carbon Dioxide on Construction Materials", SPE paper no. 4667, 1973.
[10] F.W.Schremp, G.R.Roberson, "Effect of Supercritical Carbon Dioxide on Construction Materials", Soc. Petr. Eng. J., 15, 227, 1975.
[11] A. Dugstad, "Fundamental Aspects of CO_2 Metal Loss Corrosion Part I: Mechanism", CORROSION/2006, Paper No. 06111, NACE International, Houston, 2006.
[12] K. O Kongshaug, M. Seiersten, "Baseline Experiments for the Modelling of Corrosion at High CO_2 Pressure", CORROSION/2004, Paper No. 4630, NACE International, Houston, 2004.
[13] Marion Seiersten "Material Selection for Separation, Transportation and Disposal of CO_2" CORROSION/2001, Paper no. 01042, NACE International, Houston, 2001.
[14] MultiScale 7.1 is a commercial software package from Expro Group International Ltd, for more information see: http://www.exprogroup.com/index.php?option=com_content&task=view&id=32&Itemid=50